Genes & Diseases (2023) 10, 554–567

Available online at www.sciencedirect.com

ScienceDirect

journal homepage: www.keaipublishing.com/en/journals/genes-diseases

FULL LENGTH ARTICLE

N6-methyladenosine modified LINC00901 promotes pancreatic cancer progression through IGF2BP2/MYC axis

Wan-Xin Peng [a,b,*], Fei Liu [c], Jia-Hong Jiang [d], Hang Yuan [e], Ziqiang Zhang [f], Liu Yang [g,**], Yin-Yuan Mo [b,h,***]

[a] *Department of Surgical Oncology, The Children's Hospital, Zhejiang University School of Medicine, National Research Center for Child Health, Hangzhou, Zhejiang 310052, China*
[b] *Cancer Center and Research Institute, University of Mississippi Medical Center, Jackson, MS 39216, USA*
[c] *Department of Nephrology, The Children's Hospital, Zhejiang University School of Medicine, National Research Center for Child Health, Hangzhou, Zhejiang 310052, China*
[d] *Department of Medical Oncology, Zhejiang Provincial People's Hospital, People's Hospital of Hangzhou Medical College, Hangzhou, Zhejiang 310014, China*
[e] *Department of Colorectal Surgery, Zhejiang Provincial People's Hospital, People's Hospital of Hangzhou Medical College, Hangzhou, Zhejiang 310014, China*
[f] *Department of Pulmonary Medicine, Tongji Hospital, Tongji University, Shanghai 200065, China*
[g] *Key Laboratory of Tumor Molecular Diagnosis and Individualized Medicine of Zhejiang Province, Zhejiang Provincial People's Hospital, People's Hospital of Hangzhou Medical College, Hangzhou, Zhejiang 310014, China*
[h] *Department of Pharmacology/Toxicology, University of Mississippi Medical Center, Jackson, MS 39216, USA*

Received 8 February 2022; accepted 17 February 2022
Available online 26 March 2022

KEYWORDS
IGF2BP2;
LINC00901;
MYC;
N6-methyladenosine

Abstract Accumulating evidence indicates that RNA methylation at N^6-methyladenosine (m6A) plays an important regulatory role in gene expression and aberrant mRNA m6A modification is often associated with a variety of cancers. However, little is known whether and how m6A-modification impacts long non-coding RNA (lncRNA) and lncRNA-mediated tumorigenesis, particularly in pancreatic ductal adenocarcinoma (PDAC). In the present study, we report that a previously uncharacterized lncRNA, LINC00901, promotes pancreatic cancer cell growth

* Corresponding author. Department of Surgical Oncology, the Children's Hospital, Zhejiang University School of Medicine, National Research Center for Child Health, Hangzhou, Zhejiang 310052, China.
** Corresponding author.
*** Corresponding author. Key Laboratory of Tumor Molecular Diagnosis and Individualized Medicine of Zhejiang Province, Zhejiang Provincial People's Hospital, People's Hospital of Hangzhou Medical College, Hangzhou, Zhejiang 310014, China.
E-mail addresses: pengwanxin@zju.edu.cn (W.-X. Peng), yangliuqq2003@163.com (L. Yang), ymo@umc.edu (Y.-Y. Mo).
Peer review under responsibility of Chongqing Medical University.

https://doi.org/10.1016/j.gendis.2022.02.014

modification (m6A);
PDAC;
YTHDF1

and invasion and moreover, LINC00901 is subject to m6A modification which regulates its expression. In this regard, YTHDF1 serves as a reader for the m6A modified LINC00901 and downregulates the LINC00901 level. Notably, two conserved m6A sites in LINC00901 are critical to the recognition of LINC00901 by YTHDF1. Finally, RNA sequencing (RNA-seq) and gene function analysis revealed that LINC00901 positively regulates MYC through upregulation of IGF2BP2, a known RNA binding protein that can enhance MYC mRNA stability. Together, our results suggest that there is a LINC00901-IGF2BP2-MYC axis through which LINC00901 promotes PDAC progression in an m6A dependent manner.

Introduction

Chemical modifications of RNA molecules play a critical role in the control of messenger RNA (mRNA) and non-coding RNA.[1] Over the past decades, more than 100 types of chemical modifications have been identified, and among them N^6-methyladenosine (m6A) is one of the most common, abundant, and conserved internal modification in eukaryotes RNA species.[2,3] The m6A mark is dynamically installed by m6A methyltransferases (i.e., writers), composed of METTL3 and METTL14[4] and their cofactors, and can be removed by demethylases (i.e., erasers), such as FTO and ALKBH5.[5,6] The recognition of m6A modified RNA by specific m6A-binding proteins (i.e., readers), such as YT521-B homology (YTH) family proteins, causes functional changes of the methylated RNAs, including nuclear trafficking, stability, alternative splicing, translation and RNA-protein interaction.[7–9] Thus, m6A modification impacts almost all aspects of biological processes, and dysregulation of m6A modification can lead to diverse diseases including cancers.

Pancreatic ductal adenocarcinoma (PDAC) ranks the fourth leading cause of cancer-related deaths, and it is predicted to become the second leading cause of cancer-related deaths by 2030 in the western world.[10,11] PDAC is a heterogeneous disease which harbors a variety of genomic, proteomic and epigenetic alterations resulting in tumor growth and immune escape.[12] Recent studies have suggested that epigenetic regulation involving m6A modification plays a role in occurrence of PDAC. For example, the upregulation of METTL3 not only promotes cell proliferation and invasion, but also enhances chemo- and radioresistance of pancreatic cancer cells.[13,14] RNA-seq analysis has demonstrated that upregulation of METTL3 upon cigarette smoke catalyzes the m6A modification of an oncogenic primary microRNA, miR-25, accelerating the maturation of miR-25, and thus promotes pancreatic cancer progression.[15] Moreover, a low level of demethylase ALKBH5 has been implicated in gemcitabine-resistance in PDAC.[16] These results provide first lines of evidence that m6A modification may play important roles in regulating PDAC progression. However, the underlying mechanism of how m6A modification regulates this process is still far from being understood.

While extensive studies have been carried out in m6A modification of mRNA, much less is known regarding m6A modification of long non-coding RNAs (lncRNAs). There is a paucity of information available regarding lncRNA m6A modification and its role in PDAC. Limited literature information suggests that lncRNAs, like mRNAs, can also be subject to m6A modification. For instance, the demethylation of lncRNA KCNK15-AS by ALKBH5 leads to downregulation of KCNK15-AS, which helps to inhibit PDAC cell motility.[17] Given that epigenetic regulation is one of the main mechanisms to control the expression of lncRNAs and its tissue specificity,[18] it is imperative to characterize lncRNA m6A modification in PDAC.

In the present study, we adopted methylated RNA immunoprecipitation (MeRIP) and lncRNA profiling approaches, and identified LINC00901 as an m6A-modified lncRNA in PDAC cells. We showed that LINC00901 promotes PDAC cells proliferation, survival, invasiveness and tumor growth. Importantly, YTHDF1 serves an m6A reader for the m6A-modified LINC00901 and negatively regulates its expression level. In support of this finding, there is a negative correlation between LINC00901 and YTHDF1 in clinical samples. Finally, RNA-seq and bioinformatic analyses combined with gain/loss of functional studies suggest that there is an m6A dependent LINC00901-IGF2BP2-MYC axis that drives PDAC progression.

Materials and methods

Cell lines

All cell lines in this study were obtained from American Type Culture Collection (Manassas, VA, USA). Pancreatic cancer cell line MIA PaCa-2 cells were cultured in DMEM medium (Fisher Scientific, Pittsburgh, PA, USA) supplemented with 10% FBS and 2.5% horse serum. AsPC-1 cells were maintained in RPMI-1640 (ATCC) medium supplemented with 10% FBS. 293T cells were cultured in DMEM medium supplemented with 10% FBS. All mediums contain 100 U/mL penicillin and 100 μg/mL streptomycin. The cell lines were authenticated by short tandem repeat (STR) analysis (Shanghai Biowing Applied Biotechnology, Shanghai). All cells were maintained at 37 °C in a humidified 5% CO_2 atmosphere.

Reagents

Sources of primary antibodies were as follows: m6A antibody (MABE1006) was from MilliporeSigma (St. Louis, MO,

USA); YTHDF1 (#86463), YTHDF2 (#80014), IGF2BP2 (#14672) were purchased from Cell Signaling Technology (Danvers, MA, USA); YTHDF3 (25537-1-AP) and GAPDH (60004-1-Ig) was from Proteintech (Chicago, IL, USA); MYC antibody was from Abcam (Cambridge, MA). Secondary antibodies conjugated with IRDye 800CW or IRDye 680 were purchased from LI-COR Biosciences (Lincoln, NE, USA). Streptavidin-agarose beads were from MilliporeSigma. The Protein A/G agarose beads were from Santa Cruz (Dallas, TX, USA). The high-fidelity Phusion enzyme was purchased from Fisher Scientific; PCR primers (Table S1) were purchased from Integrated DNA Technologies (Coralville, IA, USA). The EpiQuik CUT&RUN m6A RNA Enrichment (MeRIP) Kit was purchased from Epigentek (Farmingdale, NY, USA).

MeRIP and lncRNA qPCR profiling

For MeRIP assay, total RNA was isolated from MIA PaCa-2 cells and 40 μg of such RNA was directly diluted in 500 μL RIP buffer (10 mM Tris pH 7.4, 150 mM NaCl, 0.1% NP40, 100U RNase inhibitor) and incubated with anti-m6A antibody or mouse IgG on a head-over-tail rotor at 4 °C overnight. The m6A RNAs were immunoprecipitated with 30 μL Protein A/G beads for 2 h at 4 °C. After a brief spin, the beads were then washed with RIP wash buffer for 5 times. Finally, m6A RNA was extracted by phenol/chloroform method. cDNA synthesis was carried out using RevertAid™ Reverse Transcriptase (Fisher Scientific) with random primers. GAPDH and lncRNA BC200 were used as internal controls. For lncRNA profiling, we used version 2 of Human Disease-Related LncRNA Profiler (Table S1).

Construction of plasmids

For expression of LINC00901, we amplified LINC00901 from cDNA using primers LINC00901-S1m-R1-5.1 and LINC00901-S1m-BamH1-3.1 (Table S1) and then cloned into S1m tagged expression vector (Addgene #138581) which has been previously described.[19] Mutation of LINC00901 at two putative m6A sites was made by two overlapped PCR products using two pairs of primers, LINC901-S1m-R1-5.2 and LINC901-mt-3.1; LINC901-mt-5.1 and LINC901-S1m-BamH-3.1 (Table S1), and then cloned into S1m vector at EcoR I and BamH I sites. For KO of YTHDF1 or LINC00901, we made a dual gRNA construct carrying Cas9 in a lentiviral vector as described previously.[20] Sequences of gRNAs were listed in Table S1. For luciferase assays, we constructed a MYC 3′-UTR luciferase reporter in pGL3-control vector at XbaI site as previously described.[21] The high-fidelity Phusion enzyme was used to amplify DNA fragments by PCR for cloning purpose. All PCR products were verified by DNA sequencing. YTHDF1 was cloned into pCDH-Myc vector using primers YTHDF1-Myc-R1-5.1 and YTHDF1-Myc-Not1-3.1 (Table S1).

S1m-tagged RNA pulldown

Modified S1 (S1m)[22] was derived from a streptavidin-binding aptamer termed S1[23,24] that acts like biotin. Thus, the S1m tagged RNA molecules can be *in vivo* pulled down by streptavidin beads. In this case, a 10-cm dish of MIA PaCa or AsPC-1 cells infected with S1m vector or S1m-LINC00901 were harvested and then lysed with 1 ml lysis buffer containing protein inhibitors and RNase inhibitor. The supernatant was collected after centrifugation for 10 min at 4 °C and then incubated with streptavidin beads for 30 min at 4 °C to remove the background. The precleaned cell lysate was transferred to a new tube and 2% of the lysate was used as an input. The remaining lysate was incubated with streptavidin beads for 4 h at 4 °C followed by washing 5 times with ice-cold PBS. Finally, the pellet was dissolved in 30 μL 2 x SDS sample buffer, followed by SDS-PAGE and Western blot with a specific antibody.

To detect m6A modified LINC00901, we also used precipitated S1m-LINC00901 with the streptavidin beads and incubated with m6A antibody (2 μg) overnight at 4 °C with rotation. After 5 times of washes with ice cold PBS, the precipitates were resuspended in 30 μL 2 x SDS sample buffer. Finally, m6A antibody bound to S1m-LINC00901 was subject to SDS-PAGE and Western blot; the signal was detected with a secondary antibody conjugated with IRDye 680.

Quantification of S1m-tagged LINC00901 by ELISA

The S1m-tagged RNA pulldown procedure was same as above, and then the precipitated RNA was extracted by phenol-chloroform mixture. EpiQuik m6A RNA Methylation Quantification Kit (Epigentek, Farmingdale, NY, USA) was used to determine the m6A RNA methylation levels of recovered RNA following the manufacturer's instructions.

Knockout (KO) by the CRISPR approach

We knocked out LINC00901, YTHDF1, IGF2BP2 and METTL3 using CRISPR/Cas9 dual gRNA approach as described previously.[25] Two gRNAs targeting each gene was cloned into a modified LentiCRISPR v2[26] by using the optimized scaffold[27] to generate LCV2-m. All primer sequences were listed in Table S1. The lentiviral vector carrying Cas9 and dual gRNAs, driven by human U6 and mouse U6 promoter, respectively, were introduced into MIA PaCa-2 or AsPC-1 cells by infection. Three days after infection, cells were subject to puromycin selection. Then, individual colonies were manually picked and expanded in 24-well plates 2 weeks later. KO clones were identified by genomic PCR and qRT-PCR or Western bot.

Lentivirus infection

Lentivirus was packaged in 293T cells using the third generation of packaging system and the virus containing culture medium was collected 48 h after transfection and spun for 10 min at 3,000 rpm. Lentivirus infection was carried out in 6-well plates by mixing 500 μL virus supernatant +500 μl medium containing 8 μg polybrene.

Quantitative RT-PCR (qRT-PCR)

PCR was performed using a standard SYBR Green method (Bio-Rad, Hercules, CA, USA) as previously described.[28] Delta—delta Ct values were used to determine their relative expression.

Cell proliferation assay

Cell proliferation assays were carried out by MTT (3-(4,5-dimethylthiazol-2-yl)-2,5-diphenyltetrazolium bromide) assays, as previously described.[29]

Colony formation assay

For the colony formation assay, cells were seeded in 6-well plates. After 14 days, the cells were fixed with 4% PFA (Sigma) and then stained with 0.5% crystal violet. The number of colonies was countered for five representative fields. The experiments were repeated for three times.

Cell migration and invasion assay

Cell migration and invasion assays were determined using 24-well transwell inserts or matrigel transwell inserts from BD Biosciences (San Jose, CA, USA). After trypsinization, 5 $\times$ 10^4 cells were resuspended in 100 μL serum-free medium and seeded in the upper chamber, and the regular medium containing 10% FBS was placed in the lower chamber. After 20 h, cells remaining in the upper membrane surface were removed with a cotton swab, whereas the cells on the lower surface were fixed in methanol, stained with 0.5% crystal violet. For quantification, pictures for each insert were taken at 20$\times$ magnification, and the cells were counted under an optical microscope.

RNA stability assay

Cells were seeded in 12-well plates overnight, and then treated with 2 μg/mL actinomycin D (Sigma—Aldrich, USA) for various time points. Total RNA was isolated by Direct-zol RNA Miniprep Kit (Zymo, CA, USA). The RNA level for each group at the indicated time points was analyzed by qRT-PCR, calculated by delta—delta Ct and normalized by U6.

Western blot

Cells were harvested, and proteins were extracted and quantified as previously described.[30] Protein samples were separated in an SDS-PAGE gel before transferring to PVDF membrane. After probing with a primary antibody, the membrane was incubated with a secondary antibody labeled with either IRDye 800CW or IRDye 680. Finally, signal intensity was determined using the Odyssey Infrared Imaging System (LICOR Biosciences, Lincoln, NE, USA).

Luciferase assay

Luciferase assay was performed as previously described.[31] Briefly, cells were transfected with appropriate plasmids in 12-well plates, and cultured for 30 h. Then the cells were harvested and lysed for luciferase assay by using Dual-Luciferase™ Reporter Assay System (Promega, Madison, WI, USA) according to the manufacturer's protocol. Renilla luciferase was used for normalization.

Animal work

Nude (nu/nu) mice (4—5 weeks old) were purchased from Harlan Laboratories (Indianapolis, IN, USA). All animal studies were conducted in accordance with NIH animal use guidelines and a protocol approved by the UMMC Animal Care Committee. MIA PaCa-2 cells with LINC00901 overexpression or vector control (pCDH); LINC00901 KO or vector control (LCV2-m) at the exponential stage were harvested and mixed with 50% matrigel, and then injected into mice (2.5 million cells/spot) s.c. as described previously.[21] Tumor growth was measured every 4 days, starting 2 weeks after injection of tumor cells.

RNA-seq and data analysis

Total RNA was extracted by Direct-zol RNA Miniprep Kit (Zymo) following the manufacturer's procedure. The total RNA quality and quantity were analysis of Bioanalyzer 2100 and RNA 6000 Nano LabChip Kit (Agilent, CA, USA) with RIN number $>$7.0. Then the paired-end 2 $\times$ 150 bp sequencing was performed on an Illumina Hiseq 4000 platform at the LC Science (Houston, TX, USA) following the vendor's recommended protocol. Briefly, the sequence quality was verified using FastQC (http://www.bioinformatics.babraham.ac.uk/projects/fastqc/). Then, Bowtie2[32] and HISAT2[33] were employed to map reads to the genome of *homo sapiens* (Version: v96). The mapped reads of each sample were assembled using StringTie.[34] After the final transcriptome was generated, StringTie and edgeR[35] were used to estimate the expression levels of all transcripts. The differentially expressed mRNAs were selected with log2 (fold change) $>$ 1 or log2 (fold change) $<$-1 and with statistical significance (P value $<$ 0.05) by R package Ballgown.[36] The Gene Orthology (GO), and Kyoto Encyclopedia of Genes and Genomes (KEGG) enrichment analysis were performed by LC Science. The raw sequencing data related to this study (LINC00901 overexpression or knockout RNA sequencing) were available on GEO using the accession number GSE169660 and GSE169705, respectively.

Gene set enrichment analysis (GSEA)

To interpret the function of regulated genes after LINC00901 overexpression or KO, gene set enrichment analysis (GSEA) (version 4.1.0) was performed with MSigDB gene sets (h.all.v7.2.symbols.gmt) and (c2.cp.kegg.v7.4.symbols.gtm) gene sets for Hallmarks and KEGG pathways. A normalized enrichment score (NES) was calculated as the primary statistics of GSEA, and genes were ranked with the metric of absolute "signal to noise" value.

CUT&RUN m6A RNA enrichment

The assay was performed according to the manufacturer's instruction. In brief, total RNA was extracted from MIA PaCa-2 cells by RNeasy Mini Kits (Qiagen). For m6A pull-down, 10-μg RNA was used for each reaction. After immnoprecipitation, the captured RNA samples were

divided into two groups. One group was digested by proteinase K plus m6A-modified RNA digestion enzyme, the other group was only digested by proteinase K. Next, the treated RNA was purified and eluted from beads, and immediately used for qRT-PCR.

Bioinformatic analysis

Correlations between pancreatic cancer patient survival and LINC00901, YTHDF1, YTHDF2 and YTHDF3 expression from Kaplan–Meier plotter (http://kmplot.com) pan-cancer dataset was analyzed using auto best cutoff. A total of 177 pancreatic cancer samples were split in high and low groups according to the cutoff value. The hazard ratio with 95% confidence intervals and log rank *p* value was calculated and significance was set at $P < 0.05$. Microarray data of LINC00901 and YTHDF1 expression from GEO dataset (GSE16515), which included 16 pairs of pancreatic tumor was downloaded from GEO (http://www.ncbi.nlm.nih.gov/geo/).

Statistics

All quantitative data are presented as mean ± S.D. of at least three independent experiments or biological replicates. Differences between the means of two samples were analyzed by Student's *t*-test, while one-way ANOVA was used for multiple groups. Statistical analyses were performed using GraphPad Prism 8. *P* values were calculated as described in figure legends for each experiment. $P < 0.05$ was considered to be statistically significant. All data shown were representative of two or more independent experiments with similar results, unless indicated otherwise.

Results

LINC00901 is subject to an N^6-methyladenosine (m6A) modification

A large body of evidence suggests that mRNA m6A modification plays an important role in diverse human diseases including cancers,[37] however much less is known regarding m6A modification of lncRNAs. To determine the role of m6A modification of lncRNAs in pancreatic cancer, we extracted total RNA from MIA PaCa-2 cells, and then performed MeRIP assays. The enriched m6A-lncRNAs were subsequently subject to qRT-PCR profiling with primers for a focus group of lncRNAs as previously described.[38,39] We found that a number of lncRNAs were enriched by m6A antibody, and among them five lncRNAs were significantly (>2.0-fold enrichment *vs*. IgG group) enriched (Fig. 1A). LINC00901 (also called BC040587) was a top candidate and thus was chosen for further characterization. Further qRT-PCR assays confirmed the enrichment of LINC00901 in both MIA PaCa-2 and AsPC-1 cells (Fig. 1B). To further demonstrate the m6A modification of LINC00901, we performed a special reciprocal RNA precipitation. We first infected MIA PaCa-2 or AsPC-1 cells with S1m-tagged LINC00901, and then recovered S1m-tagged LINC00901 RNA by pulldown with streptavidin beads. Next, we incubated the precipitated LINC00901 with m6A antibody (mouse specific) overnight at 4 °C and precipitated again, followed by Western blot with second antibody against mouse IgG (H + L). As expected, we detected a strong signal of both heavy chain (HC) and light chain (LC) in the LINC00901-S1m lane, but only a little background in the vector control lane (Fig. 1C), further supporting that LINC00901 is methylated at m6A. Moreover, we also performed ELISA assay for such precipitated LINC00901 to measure the m6A level using EpiQuik m6A RNA Methylation Quantification Kit. Consistent with above results, we detected a higher level of m6A signal in LINC00901 group than vector control (Fig. 1D). Collectively, these results suggest that LINC00901 is m6A modified in PDAC cells.

The increased level of LINC00901 is associated with poor prognosis of pancreatic cancer patients

Of interest, analysis of PADC patients from Kaplan–Meier plotter (http://kmplot.com) pan-cancer dataset suggested that a high level of LINC00901was significantly associated with a poor prognosis in these patients for overall survival (OS) (Fig. 1E) or relapse free survival (RFS) (Fig. 1F). In support of this finding, analysis of LncExpDB database (https://bigd.big.ac.cn/lncexpdb)[40] revealed the significant high expression of LINC00901 in pancreatic cancer cell lines compared to normal pancreas cells (Fig. S1).

The oncogenic role of LINC00901 in PDAC

To define the role of m6A-regulated LINC00901 in pancreatic cancer tumorigenesis, we ectopically expressed LINC00901 in MIA PaCa-2 and AsPC-1 cells, respectively, and found that LINC00901 overexpression increased cell proliferation, as detected by MTT assays (Fig. 2A) or cell survival, as determined by colony formation assays (Fig. 2B). Furthermore, overexpression of LINC00901 promoted cell migration and cell invasion in MIA PaCa-2 (Fig. 2C) or AsPC-1 cells (Fig. 2D). Mouse xenograft model with MIA PaCa-2 cell with LINC00901 overexpression revealed that LINC00901 also significantly promoted tumor growth (Fig. 2E).

To further determine the function of LINC00901 in PDAC progression, we knocked out LINC00901 using CRISPR/Cas9 approach in MIA PaCa-2 and AsPC-1 cells. We chose two knockout (KO) clones of each cell line for further characterization. As shown in Figure 3A, LINC00901 KO caused a strong reduction of cell proliferation rate as compared with vector control. Colony formation assays showed that LINC00901 KO repressed cell survival ability (Fig. 3B). Moreover, the migration and invasion ability were significantly impaired in LINC00901 KO cells in MIA PaCa-2 or AsPC-1 cell (Fig. 3C). More importantly, rescue experiment, i.e., re-expression of LINC00901 in KO cells, restored the proliferation (Fig. S2A, B) and invasion ability (Fig. S2C, D). Finally, xenograft tumor model revealed that KO of LINC00901 significantly repressed tumor growth (Fig. 3D), in contrast to LINC00901 overexpression (Fig. 2E). These

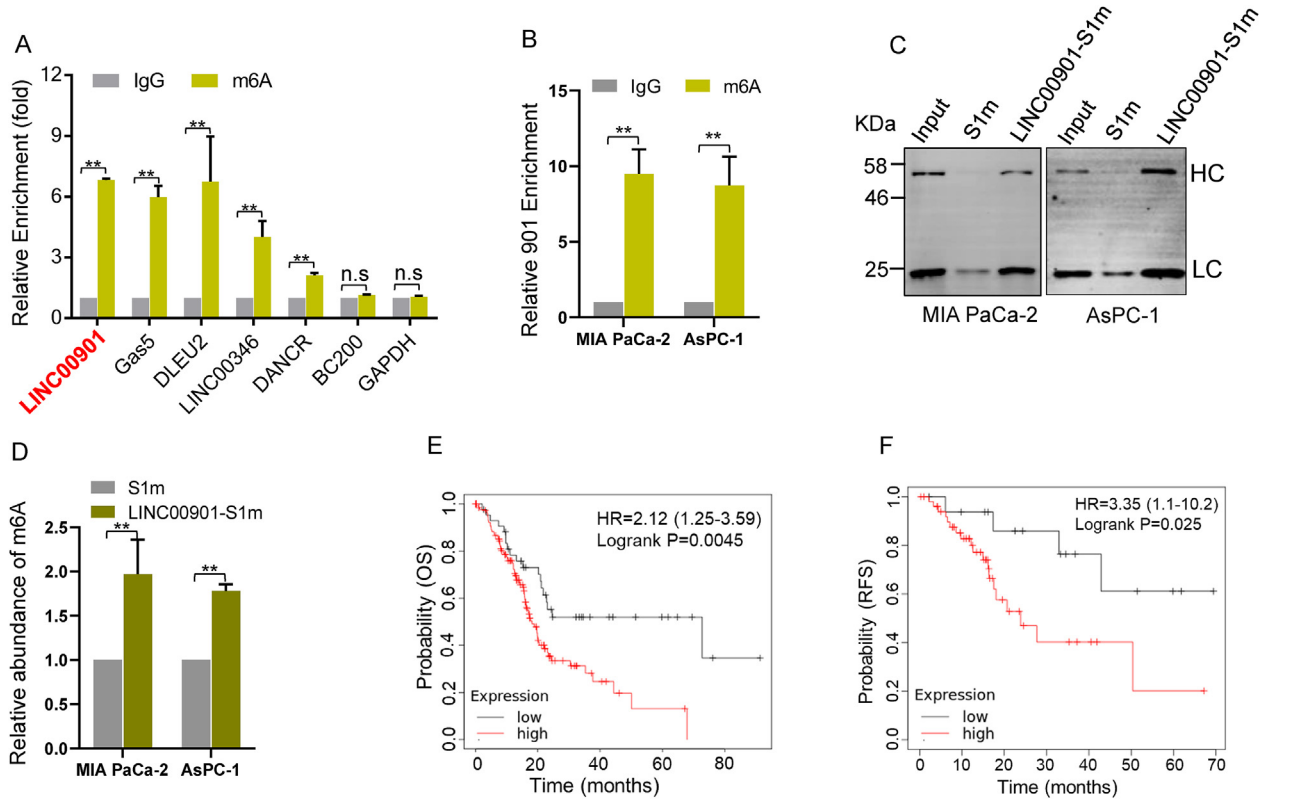

Figure 1 LINC00901 is an m6A-modified lncRNA and its high level is associated with poor prognosis of PDAC patients. **(A)** MeRIP and lncRNA profiling identified five candidate lncRNAs in MIA PaCa-2 cells, among them LINC00901 is a top candidate. BC200 and GAPDH were used as internal controls. **(B)** Validation of lncRNA profiling results in both MIA PaCa-2 and AsPC-1 cells by MeRIP and qRT-PCR assay. **(C)** Detection of interaction of LINC00901 with m6A antibody in MIA PaCa-2 and AsPC-1 cells. *In vivo* expressed S1m-tagged LINC00901 or vector control (S1m) was first pulled down by streptavidin beads and then incubated with m6A antibody overnight. The signals bound to the membrane were detected by donkey anti-mouse antibody conjugated with IRDye® 680RD. HC, heavy chain; LC, light chain. **(D)** RNA m6A methylation level of LINC00901 as determined by EpiQuik m^{6}A RNA Methylation Quantification Kit. *In vivo* expressed S1m-tagged LINC00901 or vector control (S1m) was pulled down by streptavidin beads and then the bound S1m-tagged RNA was isolated from the precipitates by phenol/chloroform extraction. The m6A level of purified RNA was measured per the manufacturer's instruction. **(E, F)** The data obtained from the Kaplan–Meier plotter database (http://kmplot.com/analysis/) suggests poor overall survival (OS) and relapse-free survival (RFS) with high expression levels of LINC00901, compared with those in the low expression levels. Values are mean ± S.D., $n = 3$, $^{**}P < 0.01$; ns, no significant.

results further support the role of LINC00901 in promoting PDAC progression.

YTHDF1 serves as a reader for m6A-modified LINC00901

To determine which readers recognize m6A-modified LINC00901, we performed *in vivo* RNA precipitation using S1m-tagged LINC00901, followed by Western blot using antibodies against YTH family proteins because the YTH family proteins are major m6A readers.[41,42] Although we tested three members of this YTH family (YTHDF1, YTHDF2 and YTHDF3), we found that only YTHDF1 interacted with LINC00901 (Fig. 4A; Fig. S3A, B). RIP assay by YTHDF1 antibody also confirmed the interaction between YTHDF1 and LINC00901, revealing >40-fold (MIA PaCa-2) or 7-fold enrichment (AsPC-1) (Fig. 4B).

To further determine the role of m6A on the interaction between LINC00901 and YTHDF1, we generated METTL3 KO in MIA PaCa-2 cells. Although METTL3 KO had no significant effect on the level of YTHDF1 (Fig. S4A), METTL3 KO abolished the enrichment of LINC00901 by YTHDF1 as compared to vector control (Fig. S4B), supporting the importance of YTHDF1 as a reader for regulation of LINC00901. We also found that METTL3 KO increased the level of LINC00901 (Fig. S4C).

Given that the recognition of target RNA by reader proteins is dependent on m6A modification, we tested the importance of the m6A modification to the interaction of LINC00901 with YTHDF1. To this end, we first identified two potential m6A modified sites (nt 286 and nt 305) in LINC00901 sequences by an online m6A site predictor program SRAMP (sequence-based RNA adenosine methylation site predictor, http://www.cuilab.cn/sramp) (Fig. S5A). Next, we took a commonly used mutagenesis approach[6,43] and generated a mutant for these two sites where "A" was mutated to "U" (Fig. S5B). This mutant (LINC00901-Mut) construct was introduced into MIA PaCa-2 and AsPC-1 cells, respectively, followed by the S1m-tagged RNA

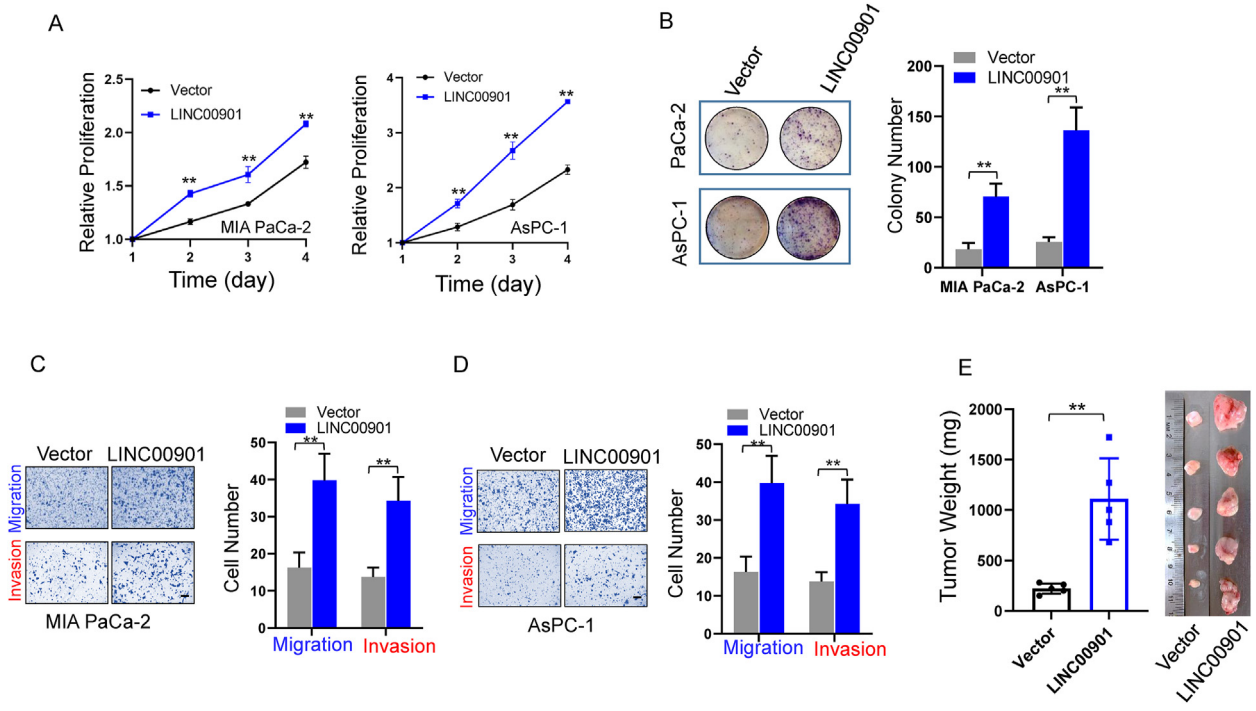

Figure 2 Effect of LINC00901 overexpression on PDAC cell proliferation, invasion and tumor growth. **(A)** Overexpression of LINC00901 promotes cell proliferation of MIA PaCa-2 (left) and AsPC-1 (right) cells, as determined by MTT assay. **(B)** Overexpression of LINC00901 increases colony formation. Left, the representative pictures of cell colony; right, quantitative results. **(C)** LINC00901 enhances migration and invasion ability of PDAC cells. Transwell assays were performed to evaluate the migration and matrigel transwell assays used to determine invasion ability following LINC00901 overexpression. **(D)** LINC00901 promotes tumor growth of MIA PaCa-2 cells. LINC00901 overexpression or vector control cells were subcutaneously injected into nude mice as described in "Materials and Methods". Tumors were harvested at the end of experiment. Left, tumor weight; right, image of tumor. Values are mean ± S.D., $n = 3$ except for (D), $^{**}P < 0.01$; bar, 100 μm.

pulldown. We also included wild type (LINC00901-WT) or vector control (S1m) in this experiment as controls. As expected, the mutation at these two sites substantially decreased the interaction between YTHDF1 and LINC00901 (Fig. 4C), suggesting that m6A modification of LINC00901 is essential to the recognition of LINC00901 by YTHDF1. In addition, MeRIP/Cut&RUN assay also suggested the important role of these potential m6A sites (Fig. S5C).

To assess the role of LINC00901 m6A modification, we introduced mutant LINC00901 (at m6A sites, see Fig. S5B) into LINC00901 KO cells. We found that both wild type and mutant LINC00901 promoted cell migration, invasion and colony formation, however, the degree of this promotion by the mutant LINC00901 was higher than the wild type LINC00901 (Fig. S6A, B). This is likely due to a higher level of mutant LINC00901 (Fig. S6C).

Recognition by YTHDF1 reduces LINC00901 stability

YTHDF1 is known to preferentially bind to m6A sites around stop codons in mRNA and the translation initiation complex, promoting translation of target mRNAs.[44] However, the function of YTHDF1 recognition in lncRNAs remains unclear. Given that m6A modification has been shown to regulate the fate of target lncRNAs by modulating its RNA stability, we determined the effect of YTHDF1 on LINC00901 level by YTHDF1 overexpression. Interestingly, ectopic expression of YTHDF1 resulted in the downregulation of LINC00901 as compared to vector control (Fig. 4D; Fig. S7A, B). In contrast, LINC00901 level was not affected by YTHDF2 or YTHDF3 (Fig. S7C, D). To further determine the effect of YTHDF1 on LINC00901 expression, we knocked out YTHDF1 in MIA PaCa-2 and AsPC-1. KO clones were identified by anti-YTHDF1 antibody immunoblotting. We found that LINC00901 level was significantly higher in MIA PaCa-2 KO cells than vector control (Fig. 4E). More importantly, re-expression of YTHDF1 in both KO clones (KO#5 and KO#9) decreased LINC00901 level (Fig. 4F). Similar results were also seen in AsPC-1 cells (Fig. S8A, B) Together, these results suggest that YTHDF1 serves as a negative regulator for LINC00901.

Next, we tested the effect of YTHDF1 on LINC00901 half-life. As shown in Figure 4G, the half-life of LINC00901 is much longer in YTHDF1 KO cells (~4 h) than in vector control cells (~2.2 h). To determine the critical role of m6A modification in the regulation of LINC00901 stability by YTHDF1, we infected MIA PaCa-2/LINC00901 KO cells (i.e., no endogenous LINC00901 background) with lentivirus expressing wild type LINC00901 (901-WT) or m6A site mutant LINC00901 (901-Mut). We found that the half-life of the mutant LINC00901 was ~3.7 h as compared to ~2.4 h for wild type LINC00901 (Fig. 4H). Moreover, MTT assay revealed that the proliferation rate for the cell carrying

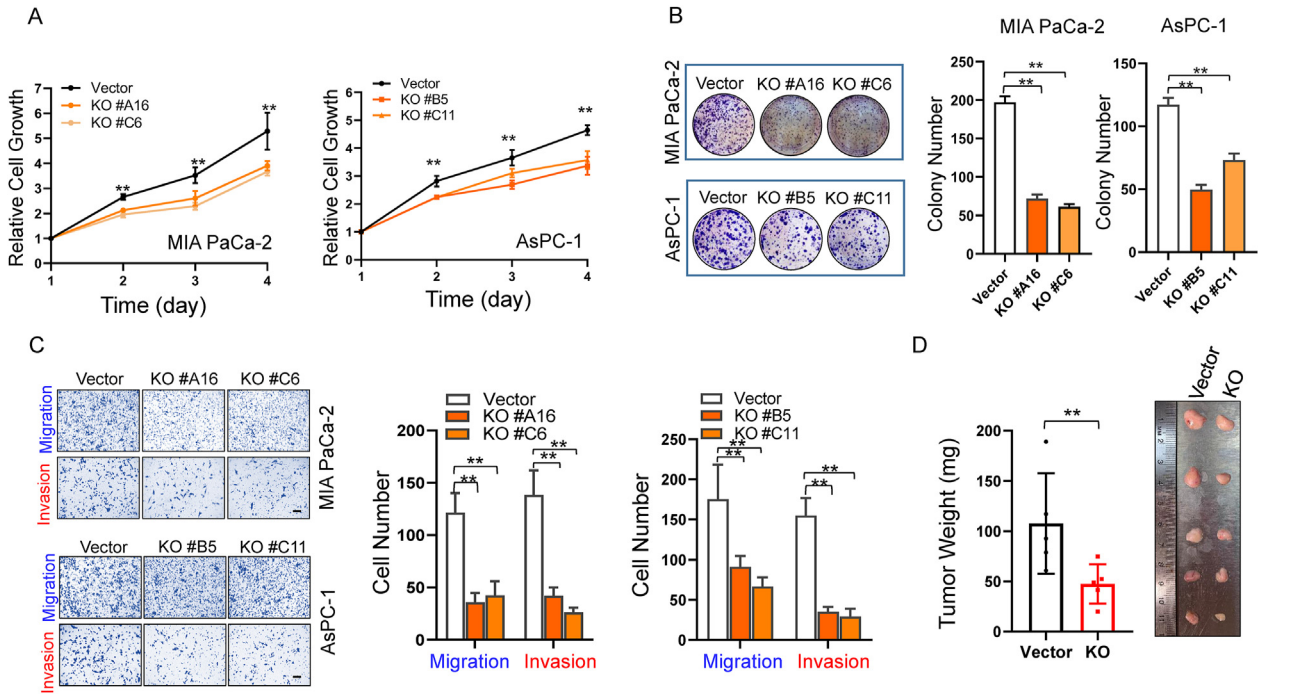

Figure 3 Effect of LINC00901 KO on PDAC cell proliferation, invasion and tumor growth. **(A)** LINC00901 KO suppresses proliferation of MIA PaCa-2 (left) or AsPC-1 (right) cells. Cell proliferation was determined by MTT assay. **(B)** LINC00901 KO causes the decrease of colony formation of MIA PaCa-2 or AsPC-1 cells. Left, the representative pictures of cell colonies; right, the quantitative data. **(C)** LINC00901 KO results in a significant decrease in cell migration or invasion potential in MIA PaCa-2 or AsPC-1 cells. **(D)** LINC00901 KO suppresses tumor growth of MIA PaCa-2 cells. Tumors were harvested at the end of experiment. Left, tumor weight; right, image of tumors. Values are mean ± S.D., $n = 3$ except for (D); $^{**}P < 0.01$; bar, 100 μm.

mutant LINC00901 was higher than that for wild type LINC00901 cells (Fig. S8C). Together, these results suggest that the recognition of m6A-modified LINC00901 by YTHDF1 accelerates LINC00901 decay.

Moreover, there was a significant negative correlation between YTHDF1 and LINC00901 expression levels in PDAC patient samples by interrogating microarray data from GEO dataset (Fig. S9A). Kaplan–Meier plot analysis showed that YTHDF1 expression level is positively associated with PDAC patient overall survival (Fig. S9B), which is contrary to the role of LINC00901 in PDAC patient's prognosis, further supporting the clinical importance of this LINC00901-YTHDF1 regulatory system.

Effect of LINC00901 on MYC expression

Having demonstrated the role of LINC00901 in PDAC and the interaction of YTHDF1 with LINC00901, we then determined how LINC00901 plays an oncogenic role. Thus, we conducted RNA sequencing (RNA-Seq) for the PDAC cells with LINC00901 overexpression or LINC00901 KO. This analysis indicated that LINC00901 overexpression resulted in the alteration of expression of 1964 mRNAs (FC|log2|≥1), while expression of 879 mRNAs was altered after LINC00901 KO. The KEGG pathway dot plots identified top 20 enrichment pathways filtered by risk factor (<0.05). Among them, the MAPK signaling pathway is a prominent enriched gene set associated with LINC00901 level in both LINC00901 overexpression and LINC00901 KO cells (Fig. 5A). GSEA analysis revealed that similar to KEGG results, LINC00901 level was positively correlated with MAPK signaling pathway (Fig. 5B). Among the 267 genes of MAPK signaling family, the oncogene *MYC* was of particular interest. Furthermore, GSEA analysis results also showed that 'MYC targets' gene set was significantly enriched in response to LINC00901 level (Fig. 5C). qRT-PCR analysis revealed that the levels of MYC target genes *CDK4*, *CDC20*, *MCM2*, *MMP3* and *SNAI2* (encoding the Slug protein) were significantly upregulated by LINC00901 overexpression (Fig. 5D); in contrast these genes were downregulated by LINC00901 KO (Fig. 5E).

To further determine the effect of LINC00901 on MYC expression, we measured the mRNA and protein expression of MYC by LINC00901 overexpression or KO. As shown in Figure 6A, levels of MYC mRNA were increased in LINC00901 overexpression cells, but were decreased in LINC00901 KO cells. Similar results were also seen at the protein level (Fig. 6B). Importantly, re-expression of LINC00901 in KO cells restored the MYC level (Fig. 6C). Furthermore, we found that LINC00901 overexpression increased MYC mRNA stability. For example, the half-life was ~20 min for vector control, but the half-life was increased to ~30 min LINC00901 overexpression (Fig. 6D). In contrast, the half-life was decreased in LINC00901 KO as compared to vector control (Fig. 6E). Luciferase assays with MYC 3′-UTR reporter showed an increased luciferase activity in LINC00901 overexpression cells (Fig. 6F, right), but a decreased luciferase activity in LINC00901 KO cells (Fig. 6F, left). These results suggest that LINC00901 positively regulates the stability of MYC mRNA.

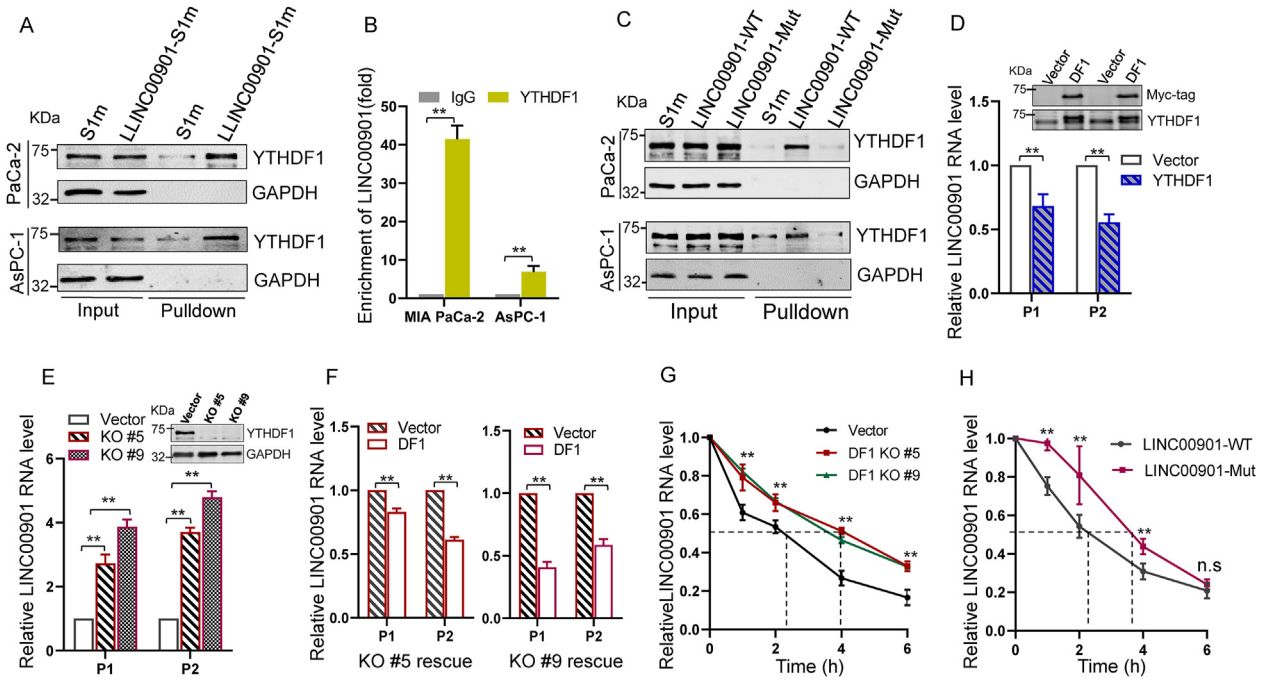

Figure 4 The recognition of m6A-modified LINC00901 by YTHDF1 suppresses LINC00901 expression. **(A)** *In vivo* RNA pulldown demonstrates that YTHDF1 binds to LINC00901. S1m-tagged LINC00901 was first introduced into MIA PaCa-2 or AsPC-1 cells by infection and then subject to *in vivo* RNA pulldown assay and Western blot with YTHDF1 antibody. **(B)** Detection of the interaction between LINC00901 and YTHDF1 in MIA PaCa-2 and AsPC-1 cells by RIP, followed by qRT-PCR. **(C)** Mutations at m6A sites abolish the interaction of LINC00901 with YTHDF1. *In vivo* S1m-tagged RNA was precipitated using MIA PaC-2 cells infected by wild type LINC00901 (901-WT), m6A mutant LINC00901 (901-Mut) or vector control. **(D)** Overexpression of YTHDF1 suppressed LINC00901 RNA expression level. MIA PaCa-2 cells were infected with YTHDF1 or vector control (pCDH). Three days after infection, total RNA was extracted and LINC00901 level was determined by qRT-PCR, P1 and P2 refer to primer sets (LINC901 RT-5.1/3.1 and LINC901-RT5.2/3.2). Upper right corner is a representative Western blot image showing the overexpression of YTHDF1. **(E)** YTHDF1 KO increases LINC00901 level. LINC00901 level was detected by qRT-PCR in YTHDF1 KO (#5 and #9) or vector control cells. Vector refers to KO vector LCV2-m. Shown in upper right corner is a representative Western blot image for YTHDF1 KO in MIA PaCa-2 KO clone#5 and #9. **(F)** Re-expression of YTHDF1 in the YTHDF1 KO cells rescues its ability to suppress LINC00901. **(G)** YTHDF1 KO enhances the stability of LINC00901. YTHDF1 KO or vector control cells were treated with actinomycin D (2 μg/ml) for indicated times, and LINC00901 level was determined by qRT-PCR. **(H)** The suppression of LINC00901 by YTHDF1 is dependent on its m6A modification. MIA PaCa-2 LINC00901 KO cell (clone #A16) were infected with 901-WT or 901-Mut. Three days after infection, the cells were treated with actinomycin D (2 μg/ml) for indicated times, and LINC00901 level was determined by qRT-PCR. Values are mean ± S.D., $n = 3$; $^{**}P < 0.01$; ns, not significant.

LINC00901 upregulates MYC through IGF2BP2

To determine whether MYC is involved in the LINC00901-mediated tumorigenesis in pancreatic cancer, we overexpressed MYC in LINC00901 KO cells. Evidently, MYC overexpression was able to rescue the LINC00901-mediated phenotypes, including increased cell proliferation (Fig. 7A), cell survival (Fig. 7B) and cell invasion (Fig. 7C). In contrast, opposite phenotype alterations were observed in LINC00901 KO#C6 cells (Fig. S10A–C).

Of interest, interrogation of the RNA-seq data revealed that IGF2BP2, an RNA binding protein which has previously been shown to enhance MYC mRNA stability,[45] was significantly altered by LINC00901 level (Fig. S11A, B). We confirmed the RNA-seq results by qRT-PCR (Fig. 7D). LINC00901 KO reduced IGF2BP2 mRNA level (Fig. 7E). At the protein level, we also found that LINC00901 overexpression increased (Fig. 7F, top), while LINC00901 KO decreased IGF2BP2 (Fig. 7F, bottom). Re-expression of LINC00901 in the LINC00901 KO cells restored IGF2BP2 protein expression (Fig. 7G). Finally, we overexpressed IGF2BP2 in LINC00901 KO cells and showed that IGF2BP2 was able to increase the MYC at both mRNA level (Fig. 7H) and protein level (Fig. 7I). To further determine the role of LINC00901 on MYC through IGF2BP2, we knocked out IGF2BP2. We found that IGF2BP2 KO caused downregulation of MYC. Next, we introduced LINC00901 into the IGF2BP2 KO cells. The result revealed that LINC00901 was still able to induce MYC in the IGF2BP2 KO background, although the degree of the MYC induction was not as great as in the IGF2BP2 background (Fig. 7L; Fig. S11C), suggesting that other factor(s) may also contribute to LINC00901-mediated MYC expression. These results suggest that LINC00901 upregulates MYC by enhancing its mRNA stability, at least in part through IGF2BP2.

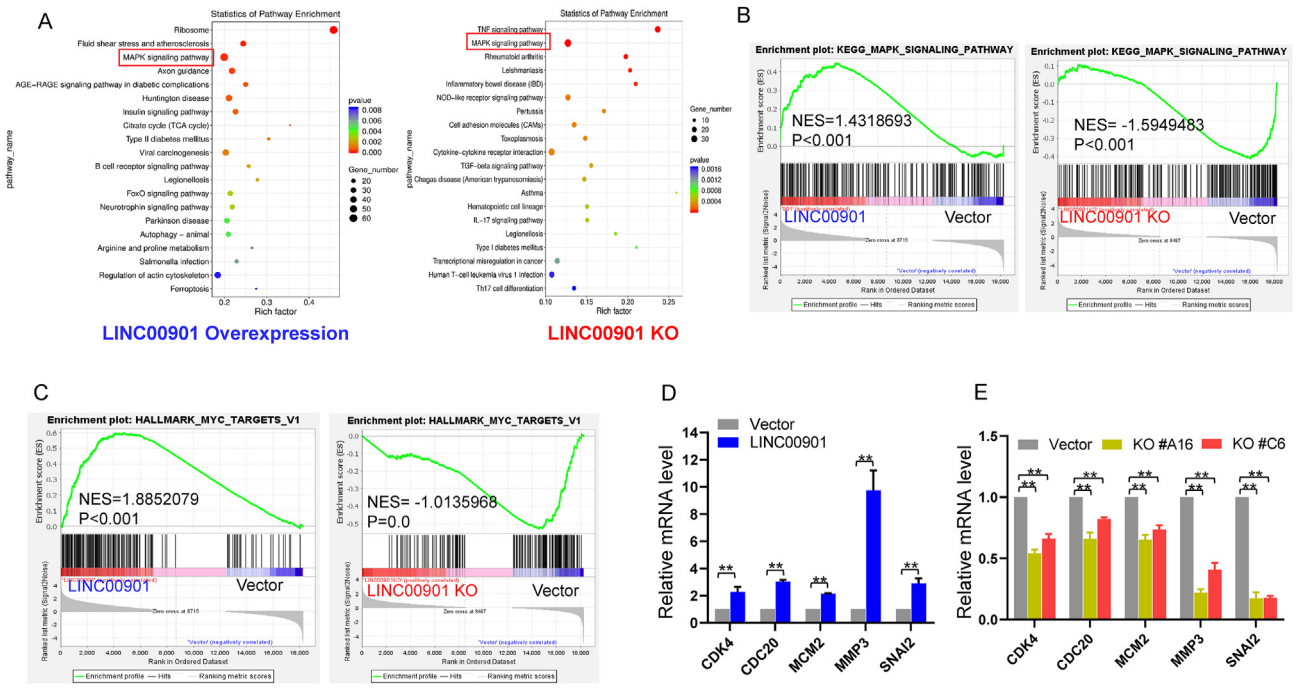

Figure 5 LINC00901 regulates MYC signaling pathway. **(A)** LINC00901 level is significantly associated with MAPK signaling pathway. Bulb map of KEGG pathway analysis of differentially expressed genes in MIA PaCa-2 LINC00901 overexpression or KO cells compared with vector control cells. X-axis represented the ratio of enriched differential genes in each pathway. Y-axis indicated names of statistics of pathway enrichment. The area of each node represented the number of enriched differential genes. The *p*-values were indicated by different color changes from blue to red. **(B)** GSEA analysis indicates that LINC00901 is involved in MAPK signaling. NES, normalized enrichment score. **(C)** Association between the enrichment of MYC targets and LINC00901 expression by GSEA analysis. **(D, E)** The expression of MYC regulated genes related to cell cycle and EMT in LINC00901 overexpression (D) or KO cells (E) was detected by qRT-PCR. Values are mean ± S.D., $n = 3$; $^{**}P < 0.01$.

Discussion

Epigenetic regulation involving m6A modification in RNA molecules can play a critical role in gene expression, and thus impact various aspects of cancer development and progression. In this regard, RNA methylation has been implicated in variety of cancers including leukemia, brain cancer, breast cancer and liver cancer. These regulators could play an oncogenic or tumor suppressive role.[46] Thus, the m6A machinery can be explored as therapeutic targets.[47,48] For instance, combination of a checkpoint inhibitor with YTHDF1 deficiency may bring extra benefits to patients with low response to checkpoint blockades.[49] In addition, the m6A modification is involved in the regulation of innate and adaptive immune cells.[50]

While intensive studies have been conducted in m6A modification of mRNA, lncRNA m6A methylation is a relatively new field. Nevertheless, increasing evidence supports the role of m6A modification of lncRNAs in cancer. For example, in colorectal cancer, m6A modification of lncRNA PR11 promotes its nuclear accumulation and thus upregulates expression of downstream gene Zeb1, driving the progression of colorectal cancer.[51] LncRNA DMDRMR interacts with IGF2BP3, stabilizing target genes such as CDK4 in an m6A-dependent manner and promoting cell proliferation in clear cell renal cell carcinoma.[52] The oncogenic function of lncRNA THOR in promoting NSCLC cell proliferation depends on its m6A modification.[53] We report herein that LINC00901 plays an oncogenic role in PDAC and it is regulated by YTHDF1 via m6A modification. Importantly, our study suggests that there is a LINC00901-IGF2BP2-MYC axis that contributes to pancreatic cancer pathogenesis.

Using MeRIP and qRT-PCR, we identify m6A modification in LINC00901, which is supported by subsequent experiments. For example, *in vivo* pulldown by S1m tagging approach, followed by m6A antibody probing, was able to show m6A modification of LINC00901 in both MIA PaCa-2 and AsPC-1 cells. Furthermore, RNA methylation quantification ELISA assay with streptavidin precipitated S1m-tagged LINC00901 detected the elevated m6A signal as compared to the control, strongly suggesting that LINC00901 is modified by m6A. By using the same mutagenesis approach as we previously did in lncRNA DANCR,[19] we were able to identify two show two conserved m6A sites critical to the interaction between LINC00901 and YTHDF1. Modification of a target (mRNA or lncRNA) may cause structural changes in such a way that different readers can recognize the m6A in a cellular content dependent manner, leading to different functional consequences. In this study, we showed that the biological function of this modification is to regulate LINC00901 level through YTHDF1 because the mutations at two conserved m6A sites in LINC00901 cause an increased half-life of LINC00901, as compared to its wild type counterpart.

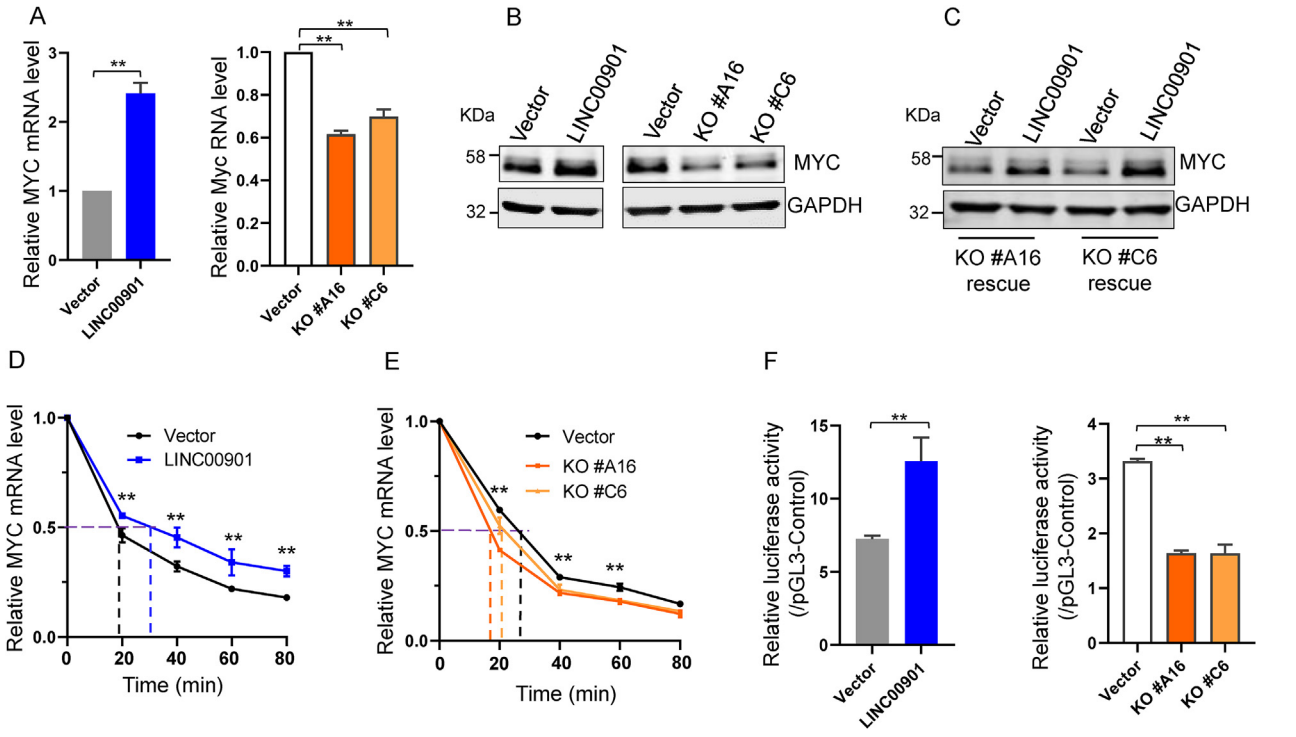

Figure 6 LINC00901 upregulates MYC. **(A)** MYC mRNA level is positively correlated with LINC00901 level. qRT-PCR was employed to determine MYC mRNA expression in LINC00901 overexpression (left) or KO (right) cells. **(B)** MYC protein level is positively correlated with LINC00901 level. Western blot was performed to test protein level of MYC in LINC00901 overexpression (left) or KO (right) cells. **(C)** Restoration of LINC00901 in KO cells rescues MYC protein expression. MYC protein level in LINC00901 re-expressed KO cells was detected by Western blot. **(D, E)** LINC00901 enhances MYC mRNA stability. LINC00901 overexpression (D) or KO (E) cells were treated with actinomycin D (2 μg/mL) for indicated times, MYC mRNA level was determined by qRT-PCR. **(F)** Luciferase reporter assay. The 3′-UTR region of MYC was cloned into pGL3-control vector as a reporter. Cells (LINC00901 overexpression or KO) were transfected with the reporter or pGL3-control vector and cultured for 30 h, then harvested for luciferase assay. Values are mean ± S.D., $n = 3$; $^{**}P < 0.01$.

It is well known that lncRNAs are frequently dysregulated in cancer, which may involve multiple mechanisms, including copy number alterations, transcription and post-transcriptional regulation. Our study suggests that m6A-mediated regulation of LINC00901 stability may also serve as an important mechanism in pancreatic cancer. In support of this notion, LINC00901 is negatively regulated by YTHDF1 in an m6A dependent manner. Furthermore, there is a negative correlation between LINC00901 and YTHDF1 in clinical specimens.

YTHDF1 belongs to a member of the YTH family proteins that have been extensively studied as m6A readers, and this family includes YTHDC1, YTHDC2, YTHDF1, YTHDF2 and YTHDF3. Although these readers share the same RNA binding domain (the ~150 amino acid YTH domain), they can play a distinct role after recognition of m6A targets in a cellular content dependent manner.[54] For example, YTHDC1 is a nuclear m6A reader that can affect splicing and export of target RNAs,[55–57] YTHDF1~3 are cytosolic readers that can impact mRNA translation and stability, and YTHDC2 can be both in nucleus and cytoplasm, but its function has not been fully elucidated.

An important function for YTHDF1 is that they can regulate protein translation[44] because vast majority m6A substrates studied so far are mRNAs. In this regard, YTHDF1 can specifically interact with m6A-modified mRNAs, facilitate ribosome loading of m6A-modified mRNAs and interact with initiation factors. As a result, it promotes their translation.[44] Subsequently, YTHDF1 has been shown to target EIF3C, a subunit of the protein translation initiation factor EIF3, in m6A dependent manner, and enhance EIF3C translation.[58] In dendritic cells, YTHDF1 recognizes m6A-modified transcripts encoding lysosomal proteases and increases the translation of lysosomal cathepsins, through which YTHDF1 is able to regulate anti-tumor immunity through mRNA m6A methylation.[49]

However, lncRNAs lack the coding capability in general. Thus, it is imperative to determine the consequence of YTHDF1 recognition in our study. Several lines of evidence suggest that the interaction of YTHDF1 with m6A-modified LINC00901 leads to a decrease in LINC00901 level through regulation of its stability, suggesting a novel aspect of YTHDF1. We first show that YTHDF1 interacts with LINC00901 by *in vivo* RNA pulldown assay. Next, we show that YTHDF1 antibody specifically precipitates LINC00901 by RIP assay. This interaction between YTHDF1 and LINC00901 depends on m6A. Mutations of these m6A sites abolish their interaction. Furthermore, YTHDF1 overexpression reduces, whereas YTHDF1 KO increases, LINC00901 level. More importantly, rescue experiments

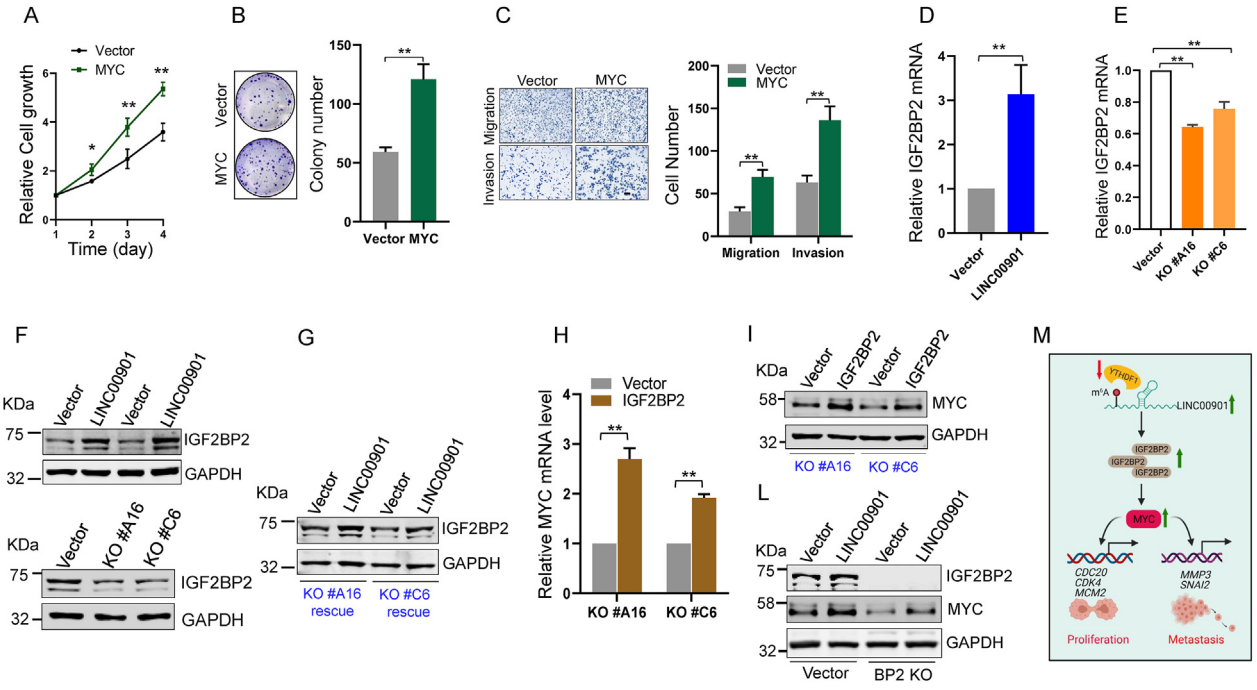

Figure 7 LINC00901 enhances MYC mRNA stability through IGF2BP2. **(A)** Overexpression of MYC in LINC00901 KO cells increases cell proliferation rate. MIA PaCa-2 LINC00901 KO cells were infected with MYC or vector control (pCDH). MTT assay was performed to determine the cell proliferation rate. **(B)** Overexpression of MYC in LINC00901 KO cells promotes cell survival, as determined by clonogenic assay. Left, image of clonogenic assay results; right, quantitative results. **(C)** Overexpression of MYC in LINC00901 KO cells promotes cell migration and invasion. **(D)** LINC00901 overexpression enhances IGF2BP2 mRNA level. **(E)** LINC00901 KO suppresses IGF2BP2 mRNA. **(F)** LINC00901 overexpression promotes (top) whereas LINC00901 KO suppresses IGF2BP2 protein level, as determined by Western blot with IGF2BP2 antibody. **(G)** Re-expression of LINC00901 in LINC00901 KO cells rescues IGF2BP2 protein level. **(H)** LINC00901 regulates MYC expression through IGF2BP2. IGF2BP2 overexpression in LINC00901 KO cells increases the mRNA. **(I)** IGF2BP2 overexpression in LINC00901 KO cells increases protein levels of MYC. **(L)** Effect of IGF2BP2 on MYC expression. IGF2BP2 KO cell were infected with LINC00901. Two days later the cells were harvested for Western blot. **(M)** The schematic model of present study. See text for discussion. Values are mean ± S.D., $n = 3$; $^{*}P < 0.05$; $^{**}P < 0.01$; bar, 100 μm.

further support the role of YTHDF1 in regulation of LINC00901. Finally, using the mutant LINC00901 along with wide type LINC00901, we show that YTHDF1 promotes LINC00901 decay in an m6A dependent manner. To our knowledge, this is the first report that YTHDF1 can promote the degradation of m6A-modified transcripts such as LINC00901.

Although a large body of studies support the importance of lncRNAs in cancer, little is known about the biological function of LINC00901, and in particular its role in pancreatic cancer. This study provides several lines of evidence that m6A-mediated LINC00901 plays an oncogenic role in pancreatic cancer. First, a high level of LINC00901 is associated with poor clinical outcomes, including overall survival and relapse free survival. Second, overexpression of LINC00901 promotes cell proliferation, cell migration and cell invasion; it also promotes tumor growth in the xenograft animal model. In contrast, LINC00901 KO reverses these phenotypes. Third, RNA-seq analysis for the cells with gain-of-function or loss-of-function of LINC00901 suggests that gene set from the MAPK signaling pathway is highly enriched, including the oncogene MYC. Fourth, LINC00901 is able to positively regulate MYC through the MYC mRNA stabilizing protein IGF2BP2. In particular, LINC00901 KO suppresses MYC, which can be rescued by re-expression of LINC00901 in the KO cells. It should be pointed out that since the level of LINC00901 detected in clinical specimens comes from total RNA, we cannot rule out other factors that may also contribute to this upregulation of LINC00901.

Regulation of MYC is complex. Evidence indicates that MYC can be regulated at various levels, including the transcriptional, posttranscriptional, translational, and post-translational levels,[59–61] in addition to amplification and translocation. Regulation of MYC by LINC00901 in this study is consistent with previous reports that lncRNAs can be also involved in regulating of MYC expression,[21,31,62–64] further supporting the complexity of this MYC regulatory system. With regard to the role of IGF2BP2 in LINC00901-mediated MYC expression, our data suggests that other factor(s) may also play a role in this aspect because LINC00901 was still able to induce MYC in the IGF2BP2 KO background. Regarding regulation of IGF2PB2 by LINC00901, since our preliminary data suggests that LINC00901 has no significant effect on IGF2PB2 mRNA stability, we speculate that transcription regulation may play a role, which warrants further investigation. Finally, detailed mechanisms as to how LINC00901 regulates MYC still remain to be determined yet.

In summary, as a potential oncogenic lncRNA, LINC00901 is regulated by m6A modification through YTHDF1 (Fig. 7M). While we have learned much about mRNA methylation in the past years, lncRNA methylation studies have just emerged as

a new frontier. Despite the similarity between protein coding genes and lncRNAs such as RNA processing, a major difference lies in their ability to produce protein. Thus, the biological consequences of their m6A methylation may also be different, particularly related to m6A readers. We show that YTHDF1 can promote LINC00901 decay via m6A modification whereas YTHDF1 is well known for its function in regulation of protein translation in mRNA m6A methylation pathway. LINC00901 upregulates IGF2BP2, which in turn enhances MYC, forming a LINC00901/IGF2BP2/MYC axis, although it still remains to be determined yet as to how LINC00901 regulates IGF2BP2. Evidently, the role of m6A modification in LINC00901 is to regulate its expression. Together, they cause PDAC cell proliferation, cell invasion and metastasis. This unique feature of YTHDF1 may provide new insight into the complex of m6A methylation in regulation of gene expression and thus could be explored for cancer therapeutic intervention.

Conflict of interests

The authors declare that they have no competing interests.

Funding

This research was supported by grants from National Natural Science Foundation of China (No. 82072703 to WP; No. 81772575 and No. 81972455 to LY), and US Department of Defense (No. CA170314 to YM).

Availability of data and materials

All data accessed from external sources have been referenced in the text and corresponding figure legends. Additional data and materials will be made available upon request.

Appendix A. Supplementary data

Supplementary data to this article can be found online at https://doi.org/10.1016/j.gendis.2022.02.014.

References

1. Song J, Yi C. Chemical modifications to RNA: a new layer of gene expression regulation. *ACS Chem Biol*. 2017;12(2):316—325.
2. Shi H, Wei J, He C. Where, when, and how: context-dependent functions of RNA methylation writers, readers, and erasers. *Mol Cell*. 2019;74(4):640—650.
3. Fu Y, Dominissini D, Rechavi G, et al. Gene expression regulation mediated through reversible m(6)A RNA methylation. *Nat Rev Genet*. 2014;15(5):293—306.
4. Liu J, Yue Y, Han D, et al. A METTL3-METTL14 complex mediates mammalian nuclear RNA N6-adenosine methylation. *Nat Chem Biol*. 2014;10(2):93—95.
5. Jia G, Fu Y, Zhao X, et al. N6-methyladenosine in nuclear RNA is a major substrate of the obesity-associated FTO. *Nat Chem Biol*. 2011;7(12):885—887.
6. Zheng G, Dahl JA, Niu Y, et al. ALKBH5 is a mammalian RNA demethylase that impacts RNA metabolism and mouse fertility. *Mol Cell*. 2013;49(1):18—29.
7. Yue Y, Liu J, He C. RNA N6-methyladenosine methylation in post-transcriptional gene expression regulation. *Genes Dev*. 2015;29(13):1343—1355.
8. Niu Y, Zhao X, Wu YS, et al. N6-methyl-adenosine (m6A) in RNA: an old modification with a novel epigenetic function. *Dev Reprod Biol*. 2013;11(1):8—17.
9. Huisman B, Manske G, Carney S, et al. Functional dissection of the m6A RNA modification. *Trends Biochem Sci*. 2017;42(2):85—86.
10. Siegel RL, Miller KD, Jemal A. Cancer statistics, 2020. *CA A Cancer J Clin*. 2020;70(1):7—30.
11. Mizrahi JD, Surana R, Valle JW, et al. Pancreatic cancer. *Lancet*. 2020;395(10242):2008—2020.
12. Grant TJ, Hua K, Singh A. Molecular pathogenesis of pancreatic cancer. *Prog Mol Biol Transl Sci*. 2016;144:241—275.
13. Xia T, Wu X, Cao M, et al. The RNA m6A methyltransferase METTL3 promotes pancreatic cancer cell proliferation and invasion. *Pathol Res Pract*. 2019;215(11):152666.
14. Taketo K, Konno M, Asai A, et al. The epitranscriptome m6A writer METTL3 promotes chemo- and radioresistance in pancreatic cancer cells. *Int J Oncol*. 2018;52(2):621—629.
15. Zhang J, Bai R, Li M, et al. Excessive miR-25-3p maturation via N(6)-methyladenosine stimulated by cigarette smoke promotes pancreatic cancer progression. *Nat Commun*. 2019;10:1858.
16. Tang B, Yang Y, Kang M, et al. M(6)A demethylase ALKBH5 inhibits pancreatic cancer tumorigenesis by decreasing WIF-1 RNA methylation and mediating Wnt signaling. *Mol Cancer*. 2020;19(1):3.
17. He Y, Hu H, Wang Y, et al. ALKBH5 inhibits pancreatic cancer motility by decreasing long non-coding RNA KCNK15-AS1 methylation. *Cell Physiol Biochem*. 2018;48(2):838—846.
18. Wang Z, Yang B, Zhang M, et al. lncRNA epigenetic landscape analysis identifies EPIC1 as an oncogenic lncRNA that interacts with MYC and promotes cell-cycle progression in cancer. *Cancer Cell*. 2018;33(4):706—720.
19. Hu X, Peng WX, Zhou H, et al. IGF2BP2 regulates DANCR by serving as an N6-methyladenosine reader. *Cell Death Differ*. 2020;27(6):1782—1794.
20. Koirala P, Huang J, Ho TT, et al. LncRNA AK023948 is a positive regulator of AKT. *Nat Commun*. 2017;8:14422.
21. Huang J, Zhang A, Ho TT, et al. Linc-RoR promotes c-Myc expression through hnRNP I and AUF1. *Nucleic Acids Res*. 2016;44(7):3059—3069.
22. Leppek K, Stoecklin G. An optimized streptavidin-binding RNA aptamer for purification of ribonucleoprotein complexes identifies novel ARE-binding proteins. *Nucleic Acids Res*. 2014;42(2):e13.
23. Srisawat C, Engelke DR. Streptavidin aptamers: affinity tags for the study of RNAs and ribonucleoproteins. *RNA*. 2001;7(4):632—641.
24. Li Y, Altman S. Partial reconstitution of human RNase P in HeLa cells between its RNA subunit with an affinity tag and the intact protein components. *Nucleic Acids Res*. 2002;30(17):3706—3711.
25. Ho TT, Zhou N, Huang J, et al. Targeting non-coding RNAs with the CRISPR/Cas9 system in human cell lines. *Nucleic Acids Res*. 2015;43(3):e17.
26. Sanjana NE, Shalem O, Zhang F. Improved vectors and genome-wide libraries for CRISPR screening. *Nat Methods*. 2014;11(8):783—784.
27. Dang Y, Jia G, Choi J, et al. Optimizing sgRNA structure to improve CRISPR-Cas9 knockout efficiency. *Genome Biol*. 2015;16:280.
28. Peng WX, Huang JG, Yang L, Gong AH, Mo YY. Linc-RoR promotes MAPK/ERK signaling and confers estrogen-independent growth of breast cancer. *Mol Cancer*. 2017;16(1):161.

29. Wu F, Chiocca S, Beck WT, et al. Gam1-associated alterations of drug responsiveness through activation of apoptosis. *Mol Cancer Therapeut*. 2007;6(6):1823—1830.
30. Sachdeva M, Wu H, Ru P, et al. microRNA-101-mediated Akt activation and estrogen-independent growth. *Oncogene*. 2011; 30(7):822—831.
31. Peng WX, He RZ, Zhang Z, et al. LINC00346 promotes pancreatic cancer progression through the CTCF-mediated Myc transcription. *Oncogene*. 2019;38(41):6770—6780.
32. Langmead B, Salzberg SL. Fast gapped-read alignment with Bowtie 2. *Nat Methods*. 2012;9(4):357—359.
33. Kim D, Langmead B, Salzberg SL. HISAT: a fast spliced aligner with low memory requirements. *Nat Methods*. 2015;12(4):357—360.
34. Pertea M, Pertea GM, Antonescu CM, et al. StringTie enables improved reconstruction of a transcriptome from RNA-seq reads. *Nat Biotechnol*. 2015;33(3):290—295.
35. Robinson MD, McCarthy DJ, Smyth GK. edgeR: a Bioconductor package for differential expression analysis of digital gene expression data. *Bioinformatics*. 2010;26(1):139—140.
36. Frazee AC, Pertea G, Jaffe AE, et al. Ballgown bridges the gap between transcriptome assembly and expression analysis. *Nat Biotechnol*. 2015;33(3):243—246.
37. Liu J, Harada BT, He C. Regulation of gene expression by N(6)-methyladenosine in cancer. *Trends Cell Biol*. 2019;29(6): 487—499.
38. Liu Q, Huang J, Zhou N, et al. LncRNA loc285194 is a p53-regulated tumor suppressor. *Nucleic Acids Res*. 2013;41(9): 4976—4987.
39. Peng WX, Koirala P, Zhang W, et al. lncRNA RMST enhances DNMT3 expression through interaction with HuR. *Mol Ther*. 2020;28(1):9—18.
40. Li Z, Liu L, Jiang S, et al. LncExpDB: an expression database of human long non-coding RNAs. *Nucleic Acids Res*. 2021;49(D1): D962—D968.
41. Wang X, Lu Z, Gomez A, et al. N6-methyladenosine-dependent regulation of messenger RNA stability. *Nature*. 2014;505(7481): 117—120.
42. Wu B, Li L, Huang Y, Ma J, Min J. Readers, writers and erasers of N(6)-methylated adenosine modification. *Curr Opin Struct Biol*. 2017;47:67—76.
43. Li N, Hui H, Bray B, et al. METTL3 regulates viral m6A RNA modification and host cell innate immune responses during SARS-CoV-2 infection. *Cell Rep*. 2021;35(6):109091.
44. Wang X, Zhao BS, Roundtree IA, et al. N(6)-methyladenosine modulates messenger RNA translation efficiency. *Cell*. 2015; 161(6):1388—1399.
45. Huang H, Weng H, Sun W, et al. Recognition of RNA N(6)-methyladenosine by IGF2BP proteins enhances mRNA stability and translation. *Nat Cell Biol*. 2018;20(3):285—295.
46. Wang S, Chai P, Jia R, et al. Novel insights on m(6)A RNA methylation in tumorigenesis: a double-edged sword. *Mol Cancer*. 2018;17(1):101.
47. Garbo S, Zwergel C, Battistelli C. m6A RNA methylation and beyond - the epigenetic machinery and potential treatment options. *Drug Discov Today*. 2021;26(11):2559—2574.
48. Nombela P, Miguel-López B, Blanco S. The role of m(6)A, m(5)C and Ψ RNA modifications in cancer: novel therapeutic opportunities. *Mol Cancer*. 2021;20(1):18.
49. Han D, Liu J, Chen C, et al. Anti-tumour immunity controlled through mRNA m 6 A methylation and YTHDF1 in dendritic cells. *Nature*. 2019;566(7743):270—274.
50. Ma Z, Gao X, Shuai Y, et al. The m6A epitranscriptome opens a new charter in immune system logic. *Epigenetics*. 2021;16(8): 819—837.
51. Wu Y, Yang X, Chen Z, et al. m(6)A-induced lncRNA RP11 triggers the dissemination of colorectal cancer cells via upregulation of Zeb1. *Mol Cancer*. 2019;18(1):87.
52. Gu Y, Niu S, Wang Y, et al. DMDRMR-mediated regulation of m(6)A-modified CDK4 by m 6 A reader IGF2BP3 drives ccRCC progression. *Cancer Res*. 2021;81(4):923—934.
53. Liu H, Xu Y, Yao B, et al. A novel N6-methyladenosine (m6A)-dependent fate decision for the lncRNA *THOR*. *Cell Death Dis*. 2020;11(8):613.
54. Yang Y, Hsu PJ, Chen YS, et al. Dynamic transcriptomic m(6)A decoration: writers, erasers, readers and functions in RNA metabolism. *Cell Res*. 2018;28(6):616—624.
55. Roundtree IA, He C. Nuclear m(6)A reader YTHDC1 regulates mRNA splicing. *Trends Genet*. 2016;32(6):320—321.
56. Xiao W, Adhikari S, Dahal U, et al. Nuclear m(6)A reader YTHDC1 regulates mRNA splicing. *Mol Cell*. 2016;61(4):507—519.
57. Roundtree IA, Luo GZ, Zhang Z, et al. YTHDC1 mediates nuclear export of N(6)-methyladenosine methylated mRNAs. *Elife*. 2017;6:e31311.
58. Liu T, Wei Q, Jin J, et al. The m6A reader YTHDF1 promotes ovarian cancer progression via augmenting EIF3C translation. *Nucleic Acids Res*. 2020;48(7):3816—3831.
59. Lu Y, Hu Z, Mangala LS, et al. MYC targeted long noncoding RNA DANCR promotes cancer in part by reducing p21 levels. *Cancer Res*. 2018;78(1):64—74.
60. Sears RC. The life cycle of C-myc: from synthesis to degradation. *Cell Cycle*. 2004;3(9):1133—1137.
61. Conacci-Sorrell M, McFerrin L, Eisenman RN. An overview of MYC and its interactome. *Cold Spring Harb Perspect Med*. 2014;4(1):a014357.
62. Maldotti M, Incarnato D, Neri F, et al. The long intergenic noncoding RNA CCR492 functions as a let-7 competitive endogenous RNA to regulate c-Myc expression. *Biochim Biophys Acta BBA Gene Regul Mech*. 2016;1859(10):1322—1332.
63. Xiao ZD, Han L, Lee H, et al. Energy stress-induced lncRNA FILNC1 represses c-Myc-mediated energy metabolism and inhibits renal tumor development. *Nat Commun*. 2017;8(1):783.
64. Hung CL, Wang LY, Yu YL, et al. A long noncoding RNA connects c-Myc to tumor metabolism. *Proc Natl Acad Sci U S A*. 2014; 111(52):18697—18702.